Radiation Physics and Chemistry 174 (2020) 108959

Contents lists available at ScienceDirect

Radiation Physics and Chemistry

journal homepage: www.elsevier.com/locate/radphyschem

Comparison between gold nanoparticles synthesized by radiolysis and by EGCG-driven gold reduction

Lucas F.de Freitas*, Cassia P.C. da Cruz, Adriana K. Cavalcante, Jorge G. dos Santos Batista, Gustavo H.C. Varca**, Monica Beatriz Mathor, Ademar B. Lugão

Instituto de Pesquisas Energéticas e Nucleares (IPEN-CNEN/SP), Av. Prof. Lineu Prestes, No 2242, Cidade Universitária, São Paulo, SP, 05508-000, Brazil

ARTICLE INFO

Keywords:
Radiolytic method
Gold nanoparticles
Green synthesis
Epigallocatechin-3-gallate

ABSTRACT

Radiolytic synthesis and phytochemical-driven gold reduction for the generation of nanoparticles are successful examples of Green Chemistry applied for nanomaterials. The present work compares these two green approaches focusing on hydrodynamic size, stability over time, optical properties and toxicity in NIH 3T3 (ATCC® CRL-1658™) cells and *Danio rerio* (Zebra Fish). The radiolytic synthesis was performed by mixing 1 mM $NaAuCl_4$; polyvinyl pyrrolidone 0.5%, $AgNO_3$ 6 × 10^{-5} M, propan-2-ol 0.2 M and acetone 0.06 M, followed by irradiation at 15 kGy (5 kGy h^{-1}, ^{60}Co source). The EGCG-functionalized nanoparticles were synthesized by mixing 1.6 mM of Au with 0.8 mM of EGCG in phosphate buffer (10 mM) for 2 h. Both methods yield the formation of gold nanoparticles featuring plasmon resonance bands at 520–530 nm, polydispersity above 0.3 was relevant only for the radiolytic protocol. Regarding stability over time, after 30 days, the nanoparticles synthesized radiolytically presented no relevant size changes, while some aggregation was observed for the EGCG-particles. The same nanoparticles demonstrated a lack of stability in high ionic strength medium. Slight toxicity was observed for the EGCG-nanoparticles in *Danio rerio*, with an IC50 calculated as 40.49%, while no IC50 was established within the concentration range of radiolysis-AuNPs used in this study. In conclusion, both green methods generated nanoparticles with good control of size and optical properties, especially via reduction by EGCG. However, the stability and toxicity results were found to be more promising for the radiolytically synthesized gold nanoparticles.

1. Introduction

Nanotechnology brings significant contributions to several areas, from catalysis to biomedical applications, and a plethora of synthetic protocols are available. Chemical protocols are based mainly on the nucleation of inorganic particles by strong or mild reducing agents, electrodeposition, interfacial polymerization, co-precipitation, microemulsion or double emulsion with solvent evaporation, and hydrothermal methods. Physical processes, on the other hand, can involve solvent radiolysis, inert gas condensation, sputtering, or even laser ablation (Kharisov et al., 2014).

The redox potential of metallic atoms is usually very negative, therefore mild reducing agents are not able to initiate the reduction of those atoms if there is no adsorption onto a surface or previously formed nanoparticles. Consequently, the chemical reduction process usually involves the use of strong, toxic reducing agents. The concern about the impact of the nanoparticles produced worldwide on the organisms and the environment has been rising, so there is an urge to apply green methods on the synthesis of nanomaterials (Belloni, Jacqueline; Mostafavi et al., 1989; Henglein, 1977; Mostafavi, Mehran; Marignier, J. L.; Amblard, J.; Belloni and Mostafavi, 2001; Shukla et al., 2008).

Radiolytic synthesis of nanoparticles is one of the successful examples of Green Chemistry (the use of non-toxic chemicals, environmentally benign solvents and renewable materials during the chemical processes), in which the reducing agents responsible for the particle nucleation are no other than the reactive species generated by the radiolysis of the solvent itself (i.e. water, acetone or alcohols). Those species, especially solvated electrons, and hydrogen radical behave as strong reducing agents and, therefore, can initiate the reduction of gold atoms and the nucleation of gold nanoparticles. The monodispersity of the resultant nanoparticles is guaranteed by the radiation dose and dose rate, as well as by the presence of size-controlling agents, such as polymers and proteins (Belloni et al., 1998).

* Corresponding author. Centro de Química e Meio Ambiente, Brazil.
** Corresponding author. Centro de Química e Meio Ambiente, Brazil.
E-mail addresses: lucasfreitas@usp.br (L.F.d. Freitas), varca@usp.br (G.H.C. Varca).

https://doi.org/10.1016/j.radphyschem.2020.108959
Received 12 August 2019; Received in revised form 24 March 2020; Accepted 1 May 2020
Available online 12 May 2020
0969-806X/

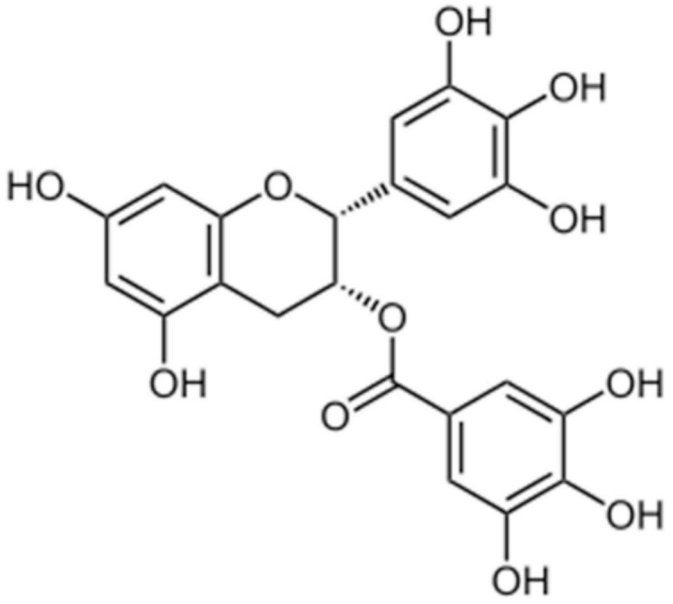

Fig. 1. Epigallocatechin-3-gallate chemical structure. The aromatic characteristic explains its property to act as a reducing agent and ROS scavenger.

Another green approach was developed by Katesh V. Katti and his team and consists of the use of phytochemicals as reducing agents for the nucleation of metallic nanoparticles. Besides reducing gold atoms, the plant-derived compounds can stabilize the nanoparticles after they are synthesized. One example of a phytochemical reducing agent in this approach is epigallocatechin-3-gallate (EGCG) (Fig. 1) which is extracted from green tea leaves. EGCG is a non-toxic, strong reducing agent and has proved to lead to size-controlled, stable and non-toxic nanoparticles, and even provides selectivity for some kinds of tumors such as prostate cancer (Katti et al., 2017).

This study consists on the comparison between these two green approaches, especially their characterization regarding hydrodynamic size (assessed by dynamic light scattering), stability over time and in different ionic strengths, optical properties (analysis of their absorption spectra from 250 to 1000 nm) and toxicity to living organisms (Zebrafish eggs and embryos (*Danio rerio*)).

2. Experimental

2.1. Materials

Polyvinyl pyrrolidone, acetone, propan-2-ol, sodium chloride, monosodium phosphate, and heptahydrate disodium phosphate were acquired from Synth (Brazil). Sodium tetrachloroaurate dehydrate and epigallocatechin-3-gallate were from Sigma-Aldrich (USA). All reagents were of analytical grade.

2.2. Methods

2.2.1. Green synthesis of gold nanoparticles

2.2.1.1. Radiolytic synthesis of gold nanoparticles. The radiolytic synthesis was performed by mixing $NaAuCl_4$ (1.0 mM), polyvinyl pyrrolidone (0.5%, 360 kDa), $AgNO_3$ (6×10^{-5} M), propan-2-ol (0.2 M), and acetone (0.06 M), followed by irradiation at 10 kGy (5 kGy h^{-1}, ^{60}Co source) in a Multipurpose Irradiator. The flasks were saturated with argon (industrial grade) and were placed in an ice bath during the irradiation to prevent an increase in temperature. After the irradiation, the resultant red suspension of gold nanoparticles was stored at 4 °C.

2.2.1.2. EGCG mediated synthesis of gold nanoparticles. Gold nanoparticles were synthesized using $NaAuCl_4$ (1.6 mM), EGCG (0.8 mM), and phosphate buffer (10 mM). The first step consisted of heating the gold solution (the salt dissolved in 9 mL of phosphate buffer) to 50 °C in glycerol bath and under magnetic stirring at 1500 rpm. Then, the EGCG dissolved in 1 mL of phosphate buffer was added to the solution, and the mixture was stirred for a further 2 min, during which the change in color is observed. Finally, the mixture is taken off the glycerol bath and left at room temperature and stirring (1500 rpm) for 12 h. The resultant nanoparticle suspension was stored at 4 °C.

2.2.2. Nanoparticle characterization

The nanoparticles were assessed for their hydrodynamic size using dynamic light scattering (DLS), zeta potential, and optical properties by spectrophotometry. The core size was measured by Transmission Electron Microscopy (TEM). Stability over time and in different ionic forces, optical properties, and toxicity in NIH 3T3 cells and *Danio rerio* embryos were also tested.

2.2.2.1. Nanoparticle size and zeta potential. Nanoparticle hydrodynamic size was estimated by dynamic light scattering (DLS) using a scattering angle of 173° at 20 °C. The samples were diluted 10 times for both the DLS analysis and zeta potential assessment. The measurements were performed in 3 sets with 10 runs of 10 s each following ISO 22412 on a Zetasizer Nano ZS90 device (Malvern Instruments, UK). The hydrodynamic diameter was reported here by number, intensity, and volume.

2.2.2.2. Nanoparticle core diameter. The nanoparticle core diameter was assessed by TEM using the Fiji imaging processing package (which includes ImageJ 1.8 software) to process the images and obtain the mean nanoparticle diameter. At least 500 nanoparticles were counted and measured with the software, and a magnification of 40,000X was applied for image acquisition. Finally, the size was calculated from the UV-VIS spectra according to Haiss et al. (2007), and all the size data were compared (Haiss et al., 2007).

2.2.2.3. Absorption spectra and stability through time and in different ionic forces. The samples were evaluated for their plasmon resonance peaks by scanning the absorbance at wavelengths ranging from 250 to 1000 nm on a SpectraMax i3 Multi-Mode spectrophotometer. The measurement was repeated 30 days after both synthesis protocols to verify the stability of the nanoparticles in suspension (stored at 4 °C).

The stability in different ionic strengths was also assessed. 100 μL of the original nanoparticles suspensions were added to 100 μL of NaCl solution in transparent 96-well plates so that the final concentrations of sodium chloride were achieved. The final concentrations investigated in this study were 0.11%, 0.225%, 0.45%, 0.9%, 1.8%, 3.6%, 7.2%, and 14.4%. The shifting of the plasmon resonance peaks was observed from 350 to 1000 nm.

2.2.2.4. Toxicity in Danio rerio. The impact on the development of Zebrafish (*Danio rerio*) embryos was investigated for different dilutions of the nanoparticles suspension (from 3.12% to 50% of nanoparticle suspension in growth medium), according to the OECD protocol nº 236 (Guideline on Fish Embryo Acute Toxicity Test – FET), as a means of assessing the possible environmental impact of the nanomaterial. An acute assay (40 organisms per concentration, 96 h of exposition to gold nanoparticles) was performed. During the test, the development of the embryos was monitored for the appearance of any malformations or dead organisms due to the presence of nanoparticles (OECD, 2013).

2.2.2.5. Cytotoxicity in NIH 3T3 cells. Murine fibroblasts (NIH 3T3 cell line) were cultured in 96-well plates, 10^4 cells per well, for 24 h with DMEM medium supplemented with 10% fetal bovine serum. Then, the medium was changed by a serum-free medium with 25% of the original gold nanoparticles suspension (v/v), and the cells were incubated with

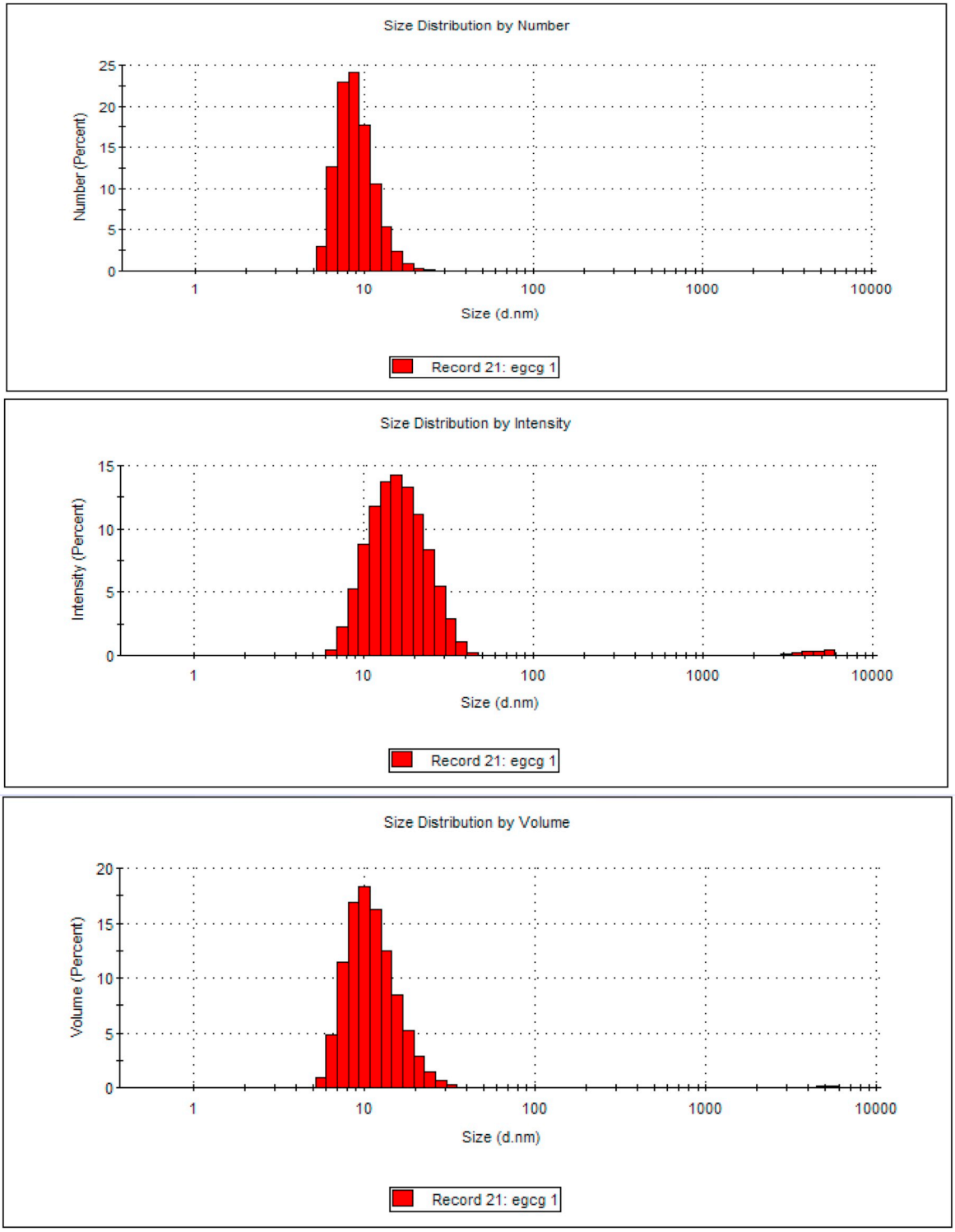

Fig. 2. The hydrodynamic size of EGCG-gold nanoparticles.

this new medium for 6 h. After this step, the wells were washed twice with sterile phosphate-buffered saline and the cells were incubated with the nanoparticle-free medium again for 24 h. Finally, the cell viability was assessed by MTS assay, and the results were compared in both synthesis protocols and to the controls (cells incubated with no nanoparticle suspension). This procedure was performed in triplicates.

2.2.2.6. Sterility testing. The nanoparticle suspensions and their controls were submitted to the sterility test before and after inoculation with *C. xerosis* to reach a 10^6 UFC mL^{-1} from a standardized *Corynebacterium xerosis* solution (ATCC® 373™) upon irradiation. Sterility assurance was tested by an independent accredited company (Controlbio Assessoria Técnica Microbiológica S/S Ltda., Brazil) using the direct inoculation assay as described in the Sterility Testing from the United States Pharmacopeia (2007) 31, NF 26 < 71 > and according to ISO 11737–2, 2009. The samples were inoculated on a culture medium and incubated for 14 days upon daily verification.

3. Results and discussion

3.1. Overview of green synthesis

Both synthesis protocols proved to be suitable for obtaining gold nanoparticles with good control in size and relative stability. However, the best size control was obtained via EGCG-driven reduction, while the most stable nanoparticles were the ones synthesized radiolytically. The results are described below.

3.1.1. EGCG-mediated synthesis of AuNP

The nanoparticles were successfully synthesized via chemical reduction by epigallocatechin-3-gallate, a phytochemical extracted from green tea leaves. This synthesis pathway led to nanoparticles with mostly 10.02 ± 2.5 nm of hydrodynamic size (as shown in the distributions by Number and Volume), but with a population of 16.97 ± 6.5 nm contributing in a significant way to the light scattering (as seen in DLS distribution by Intensity) Fig. 2). However, there is still a narrow size distribution, as confirmed by TEM images, which revealed a core size of 5.3 ± 0.6 nm (Fig. 3), and also the low polydispersity index assessed by DLS, which was around 0.186. The absorption spectrum shows the peak corresponding to plasmon resonance at 520 nm (Fig. 4). Furthermore, the zeta potential measured for these particles was 19.5 ± 1.3 mV. The size of the nanoparticles is smaller than the ones originally synthesized by Katti et al. (2017), most probably because of the heating step. It is known that the higher the temperature during the initial steps of the nanoparticle formation, the smaller the resultant gold colloids (Mountrichas et al., 2014).

The size measurements by DLS are similar to the size calculated from the UV-VIS spectra, which turned out to be 9.8 nm. The size observed in TEM does not account for the coating layer, therefore it usually tends to be smaller.

3.1.2. Radyolitic synthesis of AuNP

The nanoparticles were successfully synthesized via radiolysis in a multipurpose irradiator. This synthesis pathway led to nanoparticles with 11.14 ± 2.6 nm of hydrodynamic size (as shown in DLS distributions by Number and Volume), but with a highly disperse population with 183.5 ± 105.8 nm contributing significantly to the light scattering, as seen by DLS size distribution by intensity (Fig. 5). The high dispersity in terms of size compared to the EGCG-gold nanoparticles was confirmed by TEM images (Fig. 6), which revealed a core size of 9.8 ± 3.4 nm, and by the moderate polydispersity index assessed by DLS, which was around 0.490. The absorption spectrum shows the peak corresponding to plasmon resonance at 528 nm (Fig. 7), therefore the calculated size according to Haiss et al. (2007) was 48.6 nm.

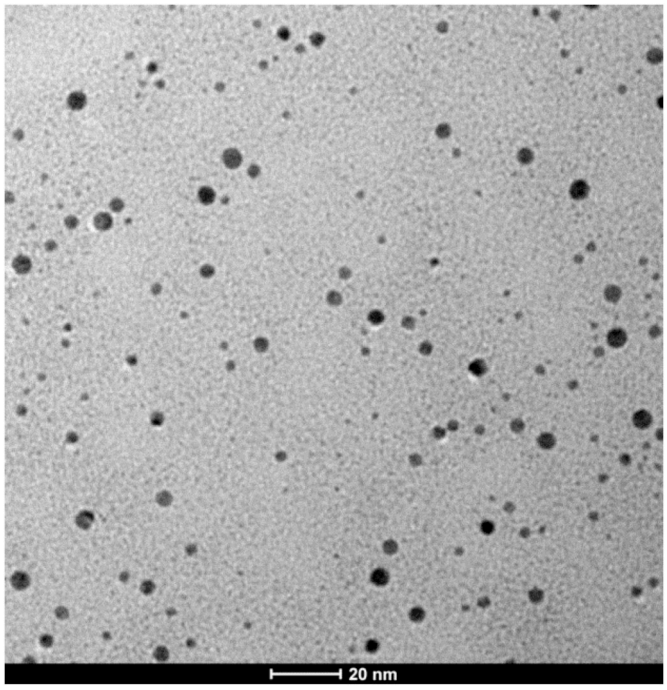

Fig. 3. TEM image of EGCG-gold nanoparticles. 40,000X magnification.

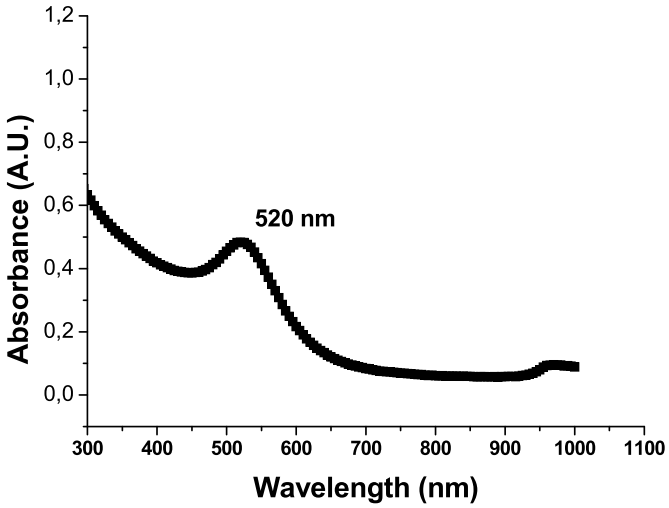

Fig. 4. The absorption spectrum of EGCG-gold nanoparticles, showing the plasmon resonance peak at 520 nm.

The discrepancies from DLS measurements are probably due to the polydispersion observed for these nanoparticles since the presence of bigger nanoparticles redshifts the plasmon resonance peak. Finally, the zeta potential measured for these particles was 31.4 ± 2.8 mV. These results are similar to the ones obtained by Misra et al. (2012), who investigated the influence of several parameters on the characteristics of the resultant gold nanoparticles. It is possible to optimize the synthesis conditions to obtain a better size and stability control.

3.1.3. Stability approach: EGCG AuNP x rad AuNP

The nanoparticles synthesized radiolytically demonstrated to be more stable through time than EGCG-gold nanoparticles, for some precipitates started to be seen in the latter nanoparticles. The absorption spectra corroborate these observations, since there is a clear change in profile, with a broadening and red-shift of the plasmon resonance peak (from 520 to 532 nm), as can be seen in Fig. 8. This indicates a size increase (Dadosh, 2009), probably due to the aggregation of the nanoparticles.

The nanoparticles synthesized via radiolysis, however, showed no change in profile, and no precipitate was observed 30 days after the synthesis (Fig. 8). The difference in the zeta potentials measured for both batches of nanoparticles (19.5 ± 1.3 mV for EGCG-gold nanoparticles and 31.4 ± 2.8 mV for radiolytically synthesized gold nanoparticles) corroborate to these observations. Thermodynamically, the colloidal system presents the smallest stability close at its isoelectric point, where all the sum of all positive and negative charges is equal to zero (consequently, the zeta potential is 0 V), but systems with zeta potential above 30 mV (positive or negative) tend to be more stable due to the charges repelling each other (Ostolska and Wiśniewska, 2014).

It is important to mention that the lower stability of EGCG-gold nanoparticles or the high size dispersion of radiolytically synthesized gold nanoparticles presented in this work are not barriers for their future use since those characteristics can be improved by simply adjusting

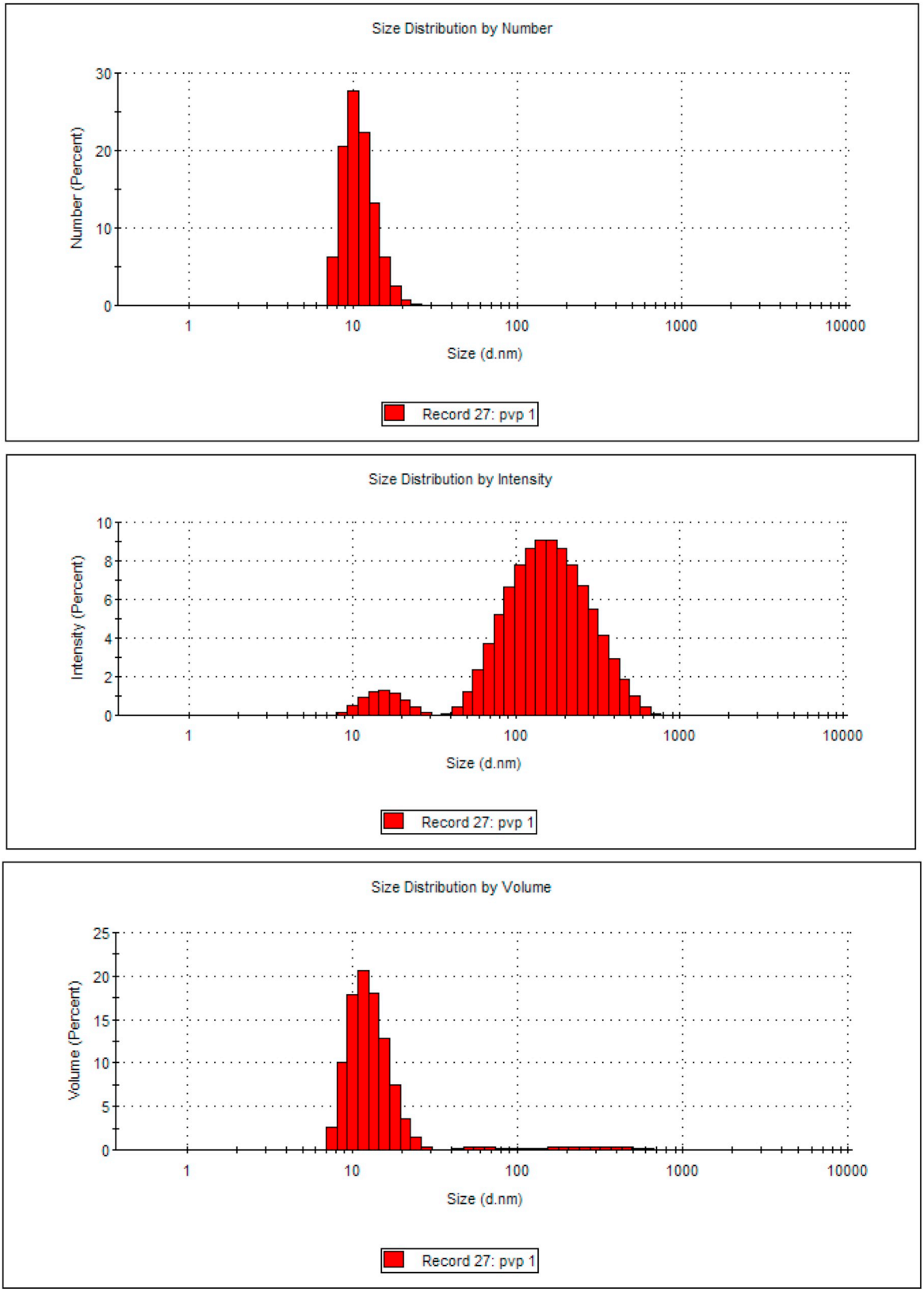

Fig. 5. The hydrodynamic size distribution of radiolytically synthesized gold nanoparticles

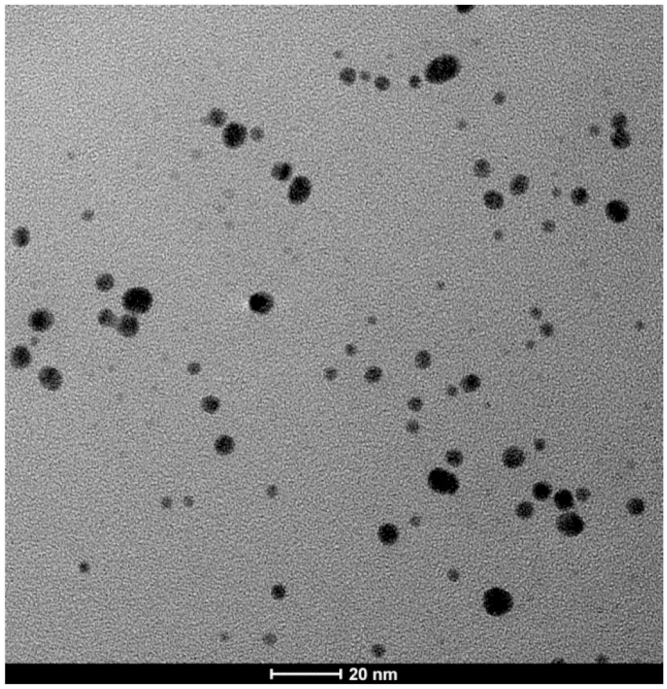

Fig. 6. TEM image of radiolytically synthesized gold nanoparticles. 40,000X magnification.

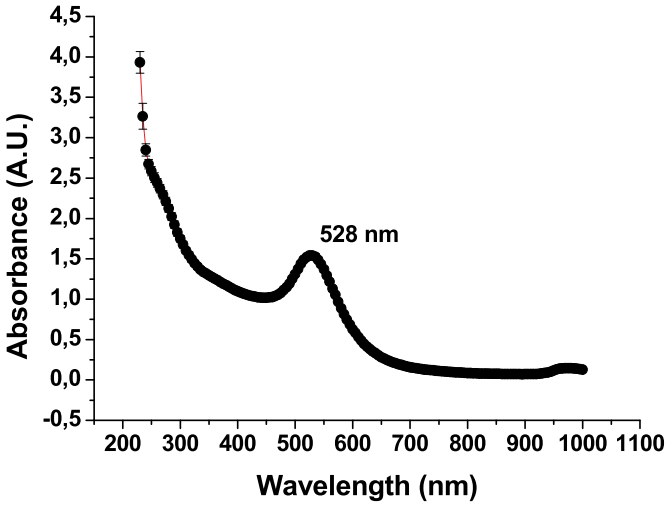

Fig. 7. The absorption spectrum of radiolytically synthesized gold nanoparticles showing the plasmon resonance peak at 528 nm.

some of the parameters used during the synthesis, which is the next step for this work in our group (Henglein and Meisel, 2002; Misra et al., 2012; Oliveira et al., 2005).

Regarding the stability in different ionic strengths, EGCG-reduced gold nanoparticles demonstrated stability up to 3.6% of NaCl (Fig. 9), while radiolytically synthesized nanoparticles were stable in all NaCl concentrations tested (Fig. 10), corroborating to the results regarding stability through time. In hypotonic media, both nanoparticles were stable.

3.1.4. Toxicity assessment in danio renio: EGCG AuNP x rad AuNP

It was not possible to calculate the IC50 for the nanoparticles synthesized by radiolysis because they presented no toxicity in any of the concentrations tested. No alterations nor malformations were observed in the embryos, and the organisms became healthy adults even in the presence of the nanoparticles (Tables 1 and 2). However, EGCG-reduced nanoparticles were moderately toxic at the highest concentrations assayed, as seen in Tables 3–5. The calculated IC50 was 40.49%. No deformities were seen in the surviving organisms, though.

3.1.5. Cytotoxicity evaluation: EGCG AuNP x radiolysis AuNP

Although there was a mild decrease in cell viability after 6 h of incubation with the nanoparticles, this difference was not significant after the statistical analysis. Therefore, all the nanoparticles tested presented no cytotoxicity to NIH 3T3 cells, corroborating to the results observed for the Zebrafish. This is in accordance with the literature regarding green gold nanoparticles, which state that the lack of toxicity presented by those biocompatible nanoparticles enables a safe delivery of this nanomaterial to the tissues and, consequently, a safe application for biomedical purposes (Nune et al., 2009). The results of the MTS cell viability assay are represented in Fig. 11.

3.1.6. Sterility testing

According to the sterility tests, the samples were produced under sterile conditions during the whole process, as the solutions before the synthesis procedures had no detectable presence of microorganisms, and the same results were obtained for the samples before and after irradiation at 10 kGy (Table 6), with regards to the radiolytic method.

As for the latter method, upon inoculation with a high load of *C. xerosis* (to reach a 10^6 CFU mL^{-1}) from a standardized solution using ATCC strain, the samples were still approved in the sterility testing, thus confirming the simultaneous nanoparticle formation and sterilization, as featured by other radiolytic methods concerning protein nanoparticles (Fazolin et al., 2020). The selection of *C. xerosis* to simulate contamination refers to the characteristics of the microorganism, Gram-positive bacteria typically found in the mucosa and normal skin microbiota (Wellinghausen, 2011).

On the other hand, as for the nanoparticles synthesized via the EGCG method, although initially identified as sterile, upon inoculation with the selected microorganism the samples were not approved in the sterility tests and thus indicated that the method was not capable of sterilizing the nanoparticles, as expected.

Therefore, the results revealed that the nanoparticles were synthesized in a sterile environment for each methodology, and the final product remained sterile after the whole process, which highlights the possible applications of the nanoparticles for biomedical purposes. However, only the radiolytic method was capable of sterilizing the nanoparticle simultaneously, even when highly-contaminated samples were used.

4. Conclusions

The particles were successfully synthesized with both protocols, with plasmon resonance band peaks ranging from 520 nm to 535 nm. The polydispersity was relevant only for the radiolytic protocol. One month after the synthesis, however, the particles synthesized with radiation had no significant size alteration, while some aggregation could be observed for the EGCG-particles. Regarding the toxicity, it was not possible to find the IC50 for the nanoparticles synthesized by radiolysis, but an IC50 of 40.49% was found for EGCG-AuNPs. Furthermore, the nanoparticles were synthesized in a sterile manner, therefore the synthesis solutions and the resultant colloids were considered sterile, and therefore, suitable for biomedical applications.

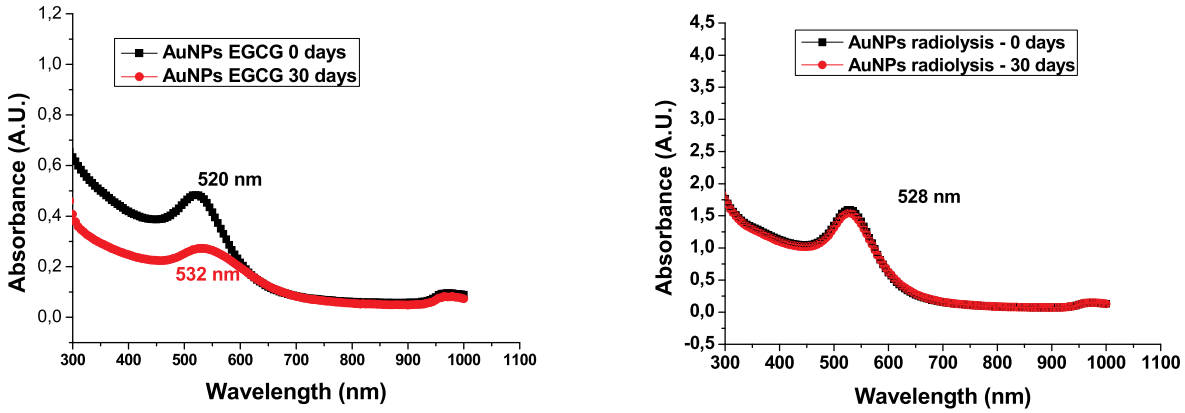

Fig. 8. Absorption spectra of gold nanoparticles synthesized by EGCG-driven reduction (left) or radiolysis (right). The black curves refer to the freshly synthesized nanoparticles, while the red curves represent the same nanoparticles after 30 days from the synthesis.

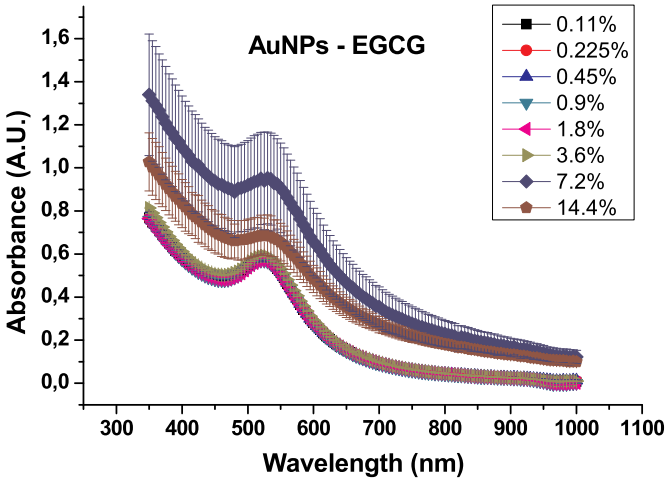

Fig. 9. Stability of EGCG-reduced gold nanoparticles in different ionic strengths (from 0.11% to 14.4% NaCl).

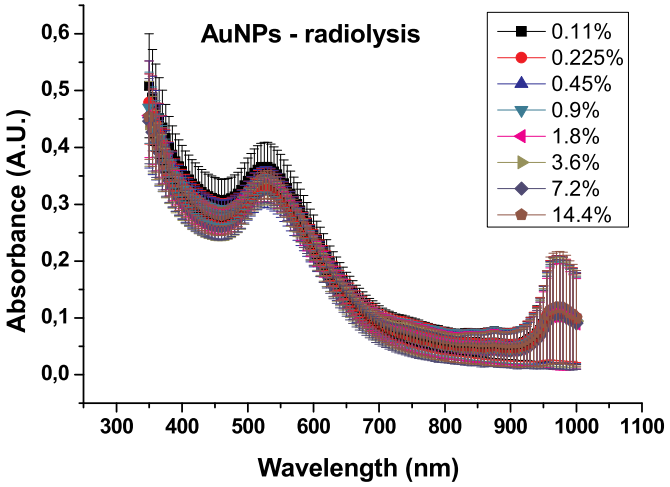

Fig. 10. Stability of radiolytically-reduced gold nanoparticles in different ionic strengths (from 0.11% to 14.4% NaCl).

Table 1
Results for the acute test on Zebrafish embryos (40 organisms per concentration, 96 h of incubation with the nanoparticles). There was no toxicity observed for the nanoparticles synthesized by radiolysis.

Concentration	Lethality
Control Murashige and Skoog (MS) medium	0 (0%)
3.12%	0 (0%)
6.25%	0 (0%)
12.5%	0 (0%)
25%	0 (0%)
50%	0 (0%)

Table 2
Sample characterization for the acute test on Zebrafish embryos using radiolysis AuNPs.

	pH	OD (mg L^{-1})
MS medium	7.0	7.9
3.12%	7.29	7.61
6.25%	7.10	7.45
12.5%	7.09	7.62
25%	7.06	7.69
50%	6.94	7.76

Table 3
Results for the acute test on Zebrafish embryos (40 organisms per concentration, 96 h of incubation with the nanoparticles). Moderate toxicity was observed for EGCG-reduced gold nanoparticles.

Concentration	Lethality
Control MS Medium	4 (10%)
3.12%	1 (2.5%)
6.25%	1 (2.5%)
12.5%	2 (5%)
25%	4 (10%)
50%	27 (67.5%)

The radiolytic method, on the other hand, was capable of providing simultaneous nanoparticle formation and sterilization under the established conditions of processing, even considering highly contaminated samples, which was not achieved by the use of EGCG.

In conclusion, these green methods of nanoparticle synthesis generate particles with good control of size and optical properties, especially via reduction by EGCG. The stability results, however, were more promising for the radiolytically synthesized gold nanoparticles. Both synthetic routes can be used, however, for biomedical applications, since they are biocompatible, environment-friendly and their characteristics can be improved by simple modifications to the synthetic parameters.

Table 4
IC50 calculated for the nanoparticles synthesized by EGCG reduction.

IC50	Confidence Interval
40.49%	95% lower confidence = 35.59% 95% upper confidence = 46.07%

Table 5
Sample characterization for the acute test on Zebrafish embryos using EGCG-AuNPs.

	pH	OD (mg L^{-1})
MS Medium	6.91	8.40
3.12%	6.93	8.28
6.25%	6.99	8.21
12.5%	7.02	8.51
25%	7.03	8.78
50%	7.05	8.81

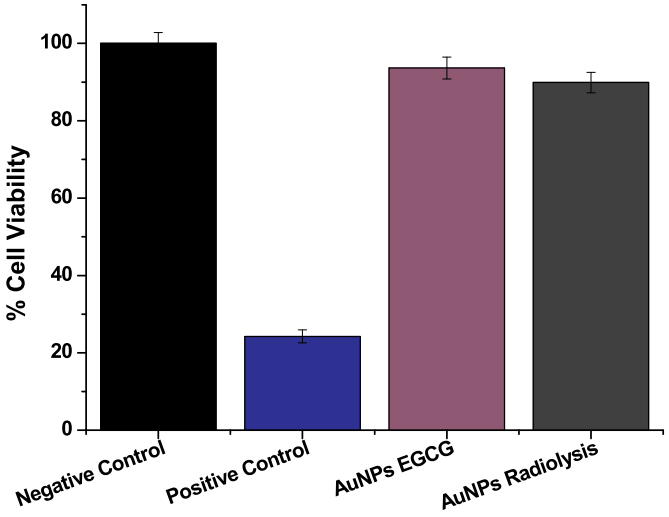

Fig. 11. Representation of the cell viability percentage assessed by MTS assay. Negative control represents cells that were not incubated with any nanoparticles, while positive control represents cells that were incubated with medium containing 25% dimethyl sulfoxide.

Table 6
Sterility testing of the AuNP's obtained by the EGCG reduction or the radiolytic method before and upon inoculation of 10^6 CFU mL^{-1} using *C. xerosis* culture.

Samples	Bacterial culture	Fungal culture	Result
AuNP's EGCG (control)	Negative	Negative	Approved
AuNP's EGCG (upon inoculation)	Positive	Negative	Reproved
AuNP's radiolysis (control)	Negative	Negative	Approved
AuNP's radiolysis (upon inoculation)	Positive	Positive	Reproved
AuNP's radiolysis (upon inoculation + 10 kGy)	Positive	Negative	Approved

*Test prepared following the ISO 11737–2.

CRediT authorship contribution statement

Lucas F.de Freitas: Writing - review & editing. **Cassia P.C. da Cruz:** Writing - review & editing. **Adriana K. Cavalcante:** Writing - review & editing. **Jorge G. dos Santos Batista:** Writing - review & editing. **Gustavo H.C. Varca:** Writing - review & editing. **Monica Beatriz Mathor:** Writing - review & editing. **Ademar B. Lugão:** Writing - review & editing.

Declaration of competing interest

The authors declare that they have no known competing financial interests or personal relationships that could have appeared to influence the work reported in this paper.

Acknowledgments

The authors would like to thank Centro de Tecnologia das Radiações (CTR – IPEN-CNEN/SP) for irradiating the samples and Instituto de Química (IQ – University of São Paulo) for the DLS analyses. Dr. Pablo Vasquez and Msc. Paulo Santos for their kind contribution to the work. Conselho Nacional de Desenvolvimento Científico e Tecnológico (CNPq) for the scholarship. International Atomic Energy Agency IAEA (CRP F22064) and CNPq for financial support (project number 402887/2013-1).

References

Belloni, Jacqueline, Mostafavi, M., 2001. Metal and semiconductor clusters. In: Jonah, C.D., Rao, M. (Eds.), Studies in Physical and Theoretical Chemistry 87. Radiation Chemistry : Present Status and Future Trends. Elsevier, pp. 446.

Belloni, J., Mostafavi, M., Remita, H., Marignier, J.-L., Delcourt, O, M., 1998. Radiation-induced synthesis of mono- and multi-metallic clusters and nanocolloids. New J. Chem. 22, 1239–1255. https://doi.org/10.1039/a801445k.

Dadosh, T., 2009. Synthesis of uniform silver nanoparticles with a controllable size. Mater. Lett. 63, 2236–2238. https://doi.org/10.1016/j.matlet.2009.07.042.

Fazolin, G.N., Varca, G.H.C., de Freitas, L.F., Rokita, B., Kadlubowski, S., Lugão, A.B., 2020. Simultaneous intramolecular crosslinking and sterilization of papain nanoparticles by gamma radiation. Radiat. Phys. Chem. 171.

Haiss, W., Thanh, N.T.K., Aveyard, J., Fernig, D.G., 2007. Determination of size and concentration of gold nanoparticles from UV - vis spectra. Anal. Chem. 79, 4215–4221. https://doi.org/10.1021/ac0702084.

Henglein, A., 1977. The reactivity of silver atoms in aqueous solutions (A γ-radiolysis study). Berichte der Bunsengesellschaft für Phys. Chemie 81, 556–561. https://doi.org/10.1002/bbpc.19770810604.

Henglein, A., Meisel, D., 2002. Radiolytic control of the size of colloidal gold nanoparticles. Langmuir 14, 7392–7396. https://doi.org/10.1021/la981278w.

Iso 11737-2, 2009. Sterilization of Medical Devices — Microbiological Methods — Part 2: Tests of Sterility Performed in the Definition, Validation and Maintenance of a Sterilization Process.

Katti, K.V., Azizi, O., Gupta, S., Katti, K.K., El-Boher, A., Duncan, R., Hubler, G., 2017. Egcg Stabilized Pd Nanoparticles, Method for Making, and Electrochemical Cell. United States Patent Application 20170009366.

Kharisov, B.I., Kharissova, O.V., Berdonosov, S.S., 2014. Radioactive nanoparticles and their main applications: recent advances. Recent Pat. Nanotechnol 79–96. https://doi.org/10.2174/1872210508021406181438 46.

Misra, N., Biswal, J., Gupta, A., Sainis, J.K., Sabharwal, S., 2012. Gamma radiation induced synthesis of gold nanoparticles in aqueous polyvinyl pyrrolidone solution and its application for hydrogen peroxide estimation. Radiat. Phys. Chem. 81, 195–200. https://doi.org/10.1016/j.radphyschem.2011.10.014.

Mostafavi, Mehran, Marignier, J.L., Amblard, J., Belloni, J., 1989. Nucleation dynamics OF silver aggregates simulation OF photographic development processes. Radiat. Phys. Chem. 34, 605–617.

Mountrichas, G., Pispas, S., Kamitsos, E.I., 2014. Effect of temperature on the direct synthesis of gold nanoparticles mediated by poly(dimethylaminoethyl methacrylate) homopolymer. J. Phys. Chem. C 118, 22754–22759. https://doi.org/10.1021/jp505725v.

Nune, S.K., Chanda, N., Shukla, R., Katti, K., Kulkarni, R.R., Thilakavathi, S.,

Mekapothula, S., Kannan, R., Katti, K.V., 2009. Green nanotechnology from tea: phytochemicals in tea as building blocks for production of biocompatible gold nanoparticles. J. Mater. Chem. 19, 2912–2920. https://doi.org/10.1039/b822015h.

Oecd, 2013. Oecd Guidelines for the Testing of Chemicals 1–22.

Oliveira, M.M., Ugarte, D., Zanchet, D., Zarbin, A.J.G., 2005. Influence of synthetic parameters on the size, structure, and stability of dodecanethiol-stabilized silver nanoparticles. J. Colloid Interface Sci. 292, 429–435. https://doi.org/10.1016/j.jcis.2005.05.068.

Ostolska, I., Wiśniewska, M., 2014. Application of the zeta potential measurements to explanation of colloidal Cr2O3stability mechanism in the presence of the ionic polyamino acids. Colloid Polym. Sci. 292, 2453–2464. https://doi.org/10.1007/s00396-014-3276-y.

Shukla, R., Nune, S.K., Chanda, N., Katti, K., Mekapothula, S., Kulkarni, R.R., Welshons, W.V., Kannan, R., Katti, K.V., 2008. Soybeans as a phytochemical reservoir for the production and stabilization of biocompatible gold nanoparticles. Small 4, 1425–1436. https://doi.org/10.1002/smll.200800525.

United States Pharmacopeia, 2007. Sterelity Test 31, 26 71.

Wellinghausen, N., Funke, Landry, 2011. Coryneform gram-positive rods. 10th. In: Manual of Clinical Microbiology, vol. 1. ASM Press, Washington, DC, pp. 413–442.